

## ANALYSIS OF MICRO-PROPERTIES FOR TRIAXIAL BEHAVIOUR ON COARSE AGGREGATES USING DEM

MAURICIO A. TAPIAS<sup>\*</sup>, EDUARDO E. ALONSO<sup>\*</sup> AND JOSEP A. GILI<sup>\*</sup>

<sup>\*</sup> Department of Geotechnical Engineering (ETSECCPB)  
Universidad Polit cnica de Catalu a  
Edificio D2, Campus Norte UPC  
Gran Capit n s/n, 08034 Barcelona, Spain  
e-mail: mauricio.tapias@upc.edu

**Key words:** Granular Materials, DEM.

**Abstract.** This paper presents an analysis of the mechanical behaviour of coarse granular aggregates using the discrete element method. A background reference for the conducted study is the set of results of a few large scale triaxial tests performed at the UPC geotechnical laboratory. The basic tool used to simulate some of the tests is the computer code PFC3D. Rockfill particles (they have the size of gravels, typically ranging from 1 cm to 4 cm) were simulated as breakable clusters of 3D balls. Particle breakage occurs in time according to fracture mechanic's laws. The relationship between stress intensity at a given particle, the size of an initial defect (crack) and the relative humidity could be established. This information was introduced in the numerical analysis to derive criteria for particle breakage in time. The paper describes the preliminary results of the work in progress. The influence of some properties such as particle shape, porosity, toughness, and friction coefficient was studied. The actual shape of rock gravels has been approximated by means of clusters of spherical particles. Several arrangements, comprising a different number of particles, have been tested, having always as reference validation criterion the results from triaxial tests performed. The results of the modelling exercise are encouraging and test results are reasonably well reproduced. The model is fairly general and it has a number of interesting capabilities.

### 1 INTRODUCTION

Coarse aggregates studied here have gravel size, typically ranging from 1 cm to 4 cm. Two different grain size distributions were studied: uniform and well-graded. In the tests performed Relative Humidity (RH) was controlled by means of a vapour equilibrium technique. The RH existing on the large pores between rock fragments controls the velocity of crack propagation within the particles. An increase in RH means a faster crack propagation and eventually the breakage of some particles and the subsequent re-arrangement of the granular structure. The results of these tests are the background reference for this study.

The paper presents the results of few numerical simulations of triaxial tests using a discrete particle method though the computer code PFC3D.

The final objective of this work is to develop a 'virtual' laboratory tool for rockfill

materials.

## 2 A MODEL FOR COARSE GRANULAR AGREGATES

A series of testing programs on gravels, performed under Relative Humidity control have stressed the relevance of particle breakage in observed macroscopic scale (Chávez & Alonso, 2003; Oldecop & Alonso, 2001; Oldecop & Alonso, 2004; Ortega, 2010). Particle breakage is controlled by the stress level, the current RH and the time.

DEM methods are potentially useful to analyze these effects. The facility to reprogram the code PFC3D through the language FISH and the ‘clump’ logic (creation of group of particles to model particle shapes) has been extensively used. In the results reported the clumps are also known as ‘macroparticles’ to distinguish them from the basic spherical particles (microparticles).

Actual particle shapes tested were formed by 4, 5, 13, and 14 microparticles (Fig. 1). The triaxial tests simulated reproduce the dimensions used in the triaxial experiments performed at UPC (Fig. 2):

- Sample size:  $\phi$ :25cm; h:50cm.
- Size of macroparticles: 3 cm. The results reported here correspond to uniform initial grain size.

Tables 1 and 2 provide some fundamental properties for the simulation.

An important practical aspect is to ensure that particles do not carry any contact force before applying the real confining stress. Clumps are generated in a random manner and a desired porosity is imposed. A relaxation of internal forces is then necessary before testing.

**Table 1.** Rockfill properties.

E (MPa)	400
n	0.4
Density (Kg/m <sup>3</sup> )	2760

**Table 2.** Properties of macroparticles in DEM model.

Normal stiffness, Kn	2e7 N/m
Shear stiffness, Ks	2e7 N/m
Friction coefficient, $\mu$	0.93 – 0.5 – 0.3

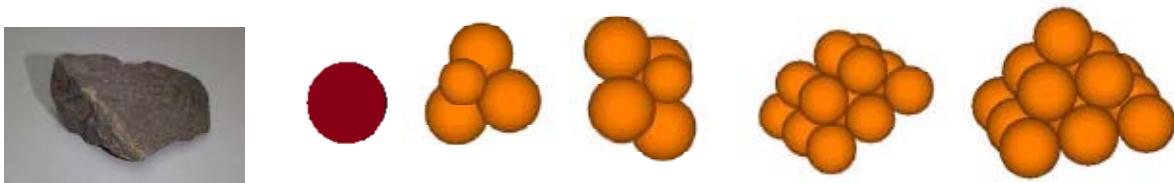


**Fig. 1.** Rockfill macroparticle. Real and clump models of 1, 4, 5, 13 and 14 microparticles.

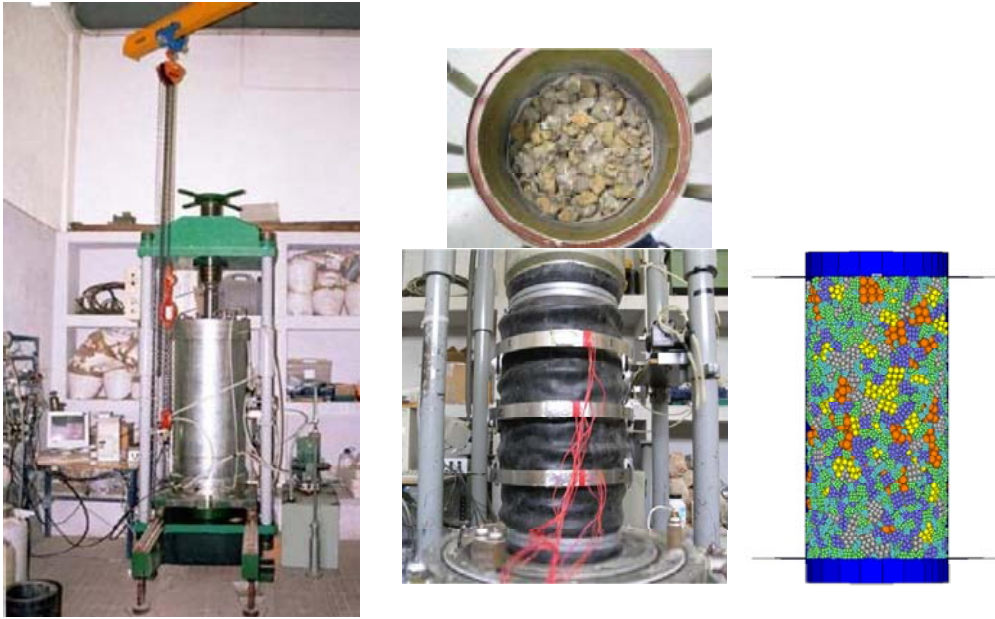


**Fig. 2.** Triaxial test on rockfill. At left, large diameter triaxial equipment of UPC geotechnical laboratory. Details of sample tested by Ortega (2010). At right, details of sample simulated.

### 3 FAILURE CRITERIA OF PARTICLES

The following issues are discussed regarding the adopted procedure to simulate particle breakage:

- Stress calculations on macroparticles
- Failure criteria for macroparticles
- Division of macroparticles

#### 3.1 Stress in macroparticles

The concept of stress is defined for a representative elementary volume –REV- (ITASCA, 2008; Bagi, 1996, 1999). The REV in our case is the macroparticle. The following procedure was implemented in the code: a) Identify the clump; b) Identify contacts with neighbouring clumps; c) Identify forces in contacts; d) Calculate the mass centroid of the clump; e) Calculate the average stress tensor through the expression (Alonso\_Marroquín & Herrman, 2005):

$$\bar{\sigma}_{ij} = \frac{1}{V} \sum_{\alpha\beta} l_i^{\alpha\beta} f_j^{\alpha\beta} \quad (1)$$

where  $l^{\alpha\beta}$ : Position vector between mass centroid and contact point;  $\alpha$  : Particle;  $\beta$  : Contact;  $V$ : Volume of macroparticle

Principal stresses are derived from the stress invariants for each macroparticle.

### 3.2 Failure criteria for macroparticles

Two failure criteria were compared: a classical Mohr Coulomb criterion and a criterion based on the propagation of cracks inside particles (Oldecop & Alonso, 2007). The second criterion is based on linear elastic fracture mechanics (LEFM).

The Mohr-Coulomb criterion requires two parameters for macroparticles: cohesion,  $c$ , and internal friction coefficient,  $\mu$ .

The crack propagation criterion is particularly useful because it allows the consideration of suction and time effects. The classical result for a mode of failure (say Mode I for failure in tension,  $\sigma$ ) specifies that whenever the stress intensity factor  $K$  reaches the toughness of the rock ( $Kc$ ) a fissure will propagate catastrophically and the rock particle will break.  $K$  is defined in terms of a characteristic size  $a$ :

$$K = \beta\sigma\sqrt{(\pi a)} \quad (2)$$

where  $\beta$  is a dimensionless coefficient which depends on particle geometry.

However, a subcritical propagation of fractures, when  $K < Kc$ , is also possible (Atkinson, 1984 ; Oldecop & Alonso 2001). Oldecop and Alonso (2007) describe a phenomenological model, based on subcritical crack growth, for the time to reach particle breakage. The model includes the effects of suction and time.

The approach followed here is to assign a random distribution of defects (cracks) to the macroparticles. Crack length follows a given statistical distribution. The factor  $K$ , which increases as the crack propagates, is calculated for the minor principal stress which corresponds to a tension state.  $K$  for each macroparticle increases also with the applied external stress to the sample tested.

For every time instant of calculation,  $K$  is compared with  $Kc$ . Whenever  $K \geq Kc$  the particle is broken in two parts. This is the phenomenon included in all the simulations reported here.

### 3.3 Particle division

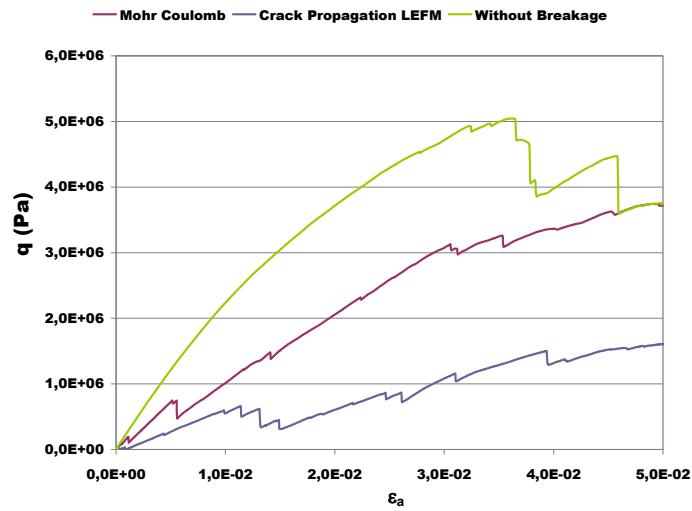
The particle division follows an arbitrary criterion which takes into account the number of particles integrating a clump and the ‘pyramidal’ structure of the macroparticle. Clumps are divided following the ‘rule’: 13→9+4; 9→5+4; 5→3+2; 4→2+2; 3→2+1; 2→1+1.

Figure 3 provides a comparison of the two criteria (Mohr Coulomb and LEFM) together with a case of no particle breakage. The simulated triaxial test exhibits the highest strength when no particles break, followed by the Mohr Coulomb rupture criterion.

## 4 SIMULATED TRIAXIAL TESTS

### 4.1 Particle Shape

Clump sizes of 1; 4(3+1); 5(4+1); 13(9+4); 14(9+4+1), which try always to simulate a pyramidal shape, were tested. Some results are given in Figure 4. The highest peak strengths are found for the highest number of particles in a clump.



**Fig. 3.** Breakage criteria effect on deviatoric behaviour. Comparison among different criteria: No breakage; crack propagation based on LEFM and Mohr Coulomb. Sample of 100 macroparticles using clumps of 13 microparticles. Confining stress: 0.5MPa

## 4.2 Porosity

The effect of two porosities (51% and 61%) on triaxial test results is given in Figure 5. In both cases the initial macroparticle system had no initial contact forces.

The sample exhibiting the lower porosity resulted in the higher stiffness, a consistent result with experimental observations. However, similar peak strength was calculated for the two specimens, a result which is probably explained by particle breakage.

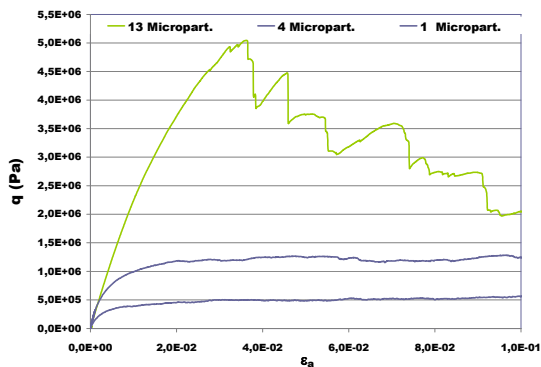


**Fig. 4.** Shape effects. Results of numerical simulation of triaxial test using macroparticles of 1, 4, and 13 microparticles. Confining stress 0.5 MPa.

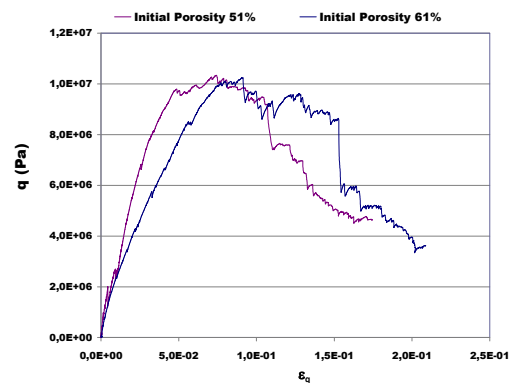


**Fig. 5.** Initial porosity effect. Comparison between two different initial porosities, 51 % y 61%. Confining stress 1.0 MPa. Sample of 1000 clumps of 14 microparticles.

### 4.3 Contact Stiffness

Three samples having particle to particle normal stiffnesses  $k_n$  equal to  $2e6$ ,  $2e7$ , and  $2e8$  N/m respectively were tested in a triaxial experiment. All particles have friction coefficient ( $\mu$ ) equal to 0.3 ( $\phi = 17^\circ$ ). Initial porosity was 51%, the initial confining stress 1 MPa and the toughness of macroparticles was  $1e4$  Pa $\sqrt{m}$ . The specimen was defined by 970 macroparticles and the initial equivalent diameter was 2.8cm.

Figure 6 shows the deviatoric stress-strain relationship. Samples with greater contact stiffnesses in the micro level (particle to particle) have greater stiffnesses at the macro level, and they get higher peak strenghts.

Dilatancy is shown in Figure 7. As expected, dilatancy increases with contact stiffness. This effect is reflected also on the change in porosity during testing (Fig. 8).

The sample having the smallest  $k_n$  exhibited a higher number of failed clumps. This sample had the lowest of number of not broken clumps (Fig. 9). This is reflected on the calculated grain size distribution at the end of the test (Fig. 10). Crushing in these samples result in an increase in particles having a equivalent diameter close to 2cm and 2.6cm.

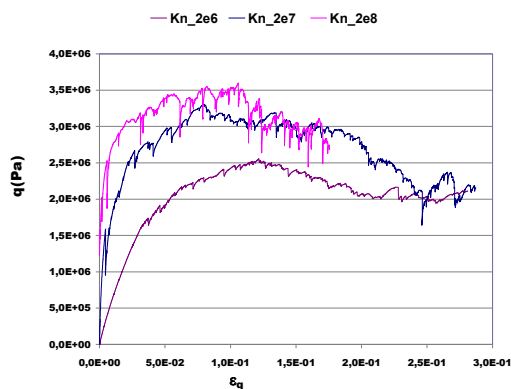


**Fig. 6.** Effect of contact stiffness on deviatoric behaviour. Comparison among three different normal stiffness ( $2e6$ ,  $2e7$ ,  $2e8$  N/m). Sample of 1000 macroparticles using clumps of 14 microparticles . Confining stress: 1.0MPa. Initial porosity: 51%.

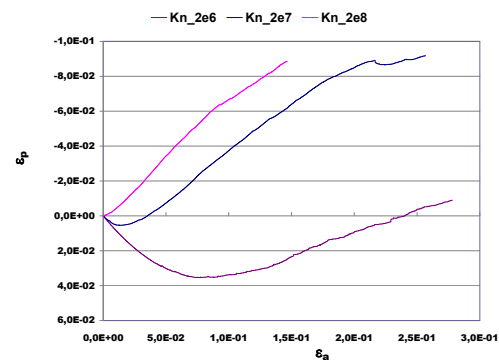


**Fig. 7.** Effect of contact stiffness on volumetric behaviour. Comparison among three different normal stiffness ( $2e6$ ,  $2e7$ ,  $2e8$  N/m). Sample of 1000 macroparticles using clumps of 14 microparticles . Confining stress: 1.0MPa. Initial porosity: 51%.

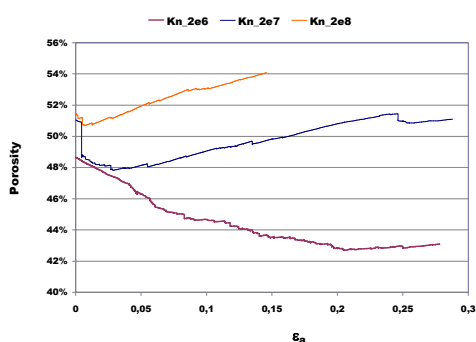


**Fig. 8.** Effect of contact stiffness on the porosity. Comparison among three different normal stiffness (2e6, 2e7, 2e8 N/m). Sample of 1000 macroparticles using clumps of 14 microparticles . Confining stress: 1.0MPa. Initial porosity: 51%.

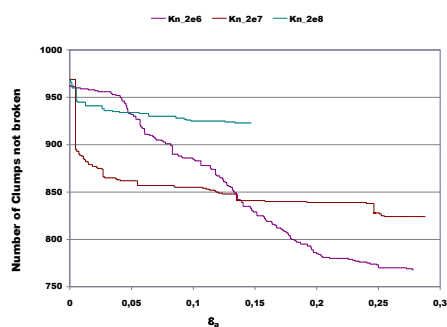


**Fig. 9.** Effect of contact stiffness on number of clumps not broken. Comparison among three different normal stiffness (2e6, 2e7, 2e8 N/m). Sample of 1000 macroparticles using clumps of 14 microparticles . Confining stress: 1.0MPa. Initial porosity: 51%.

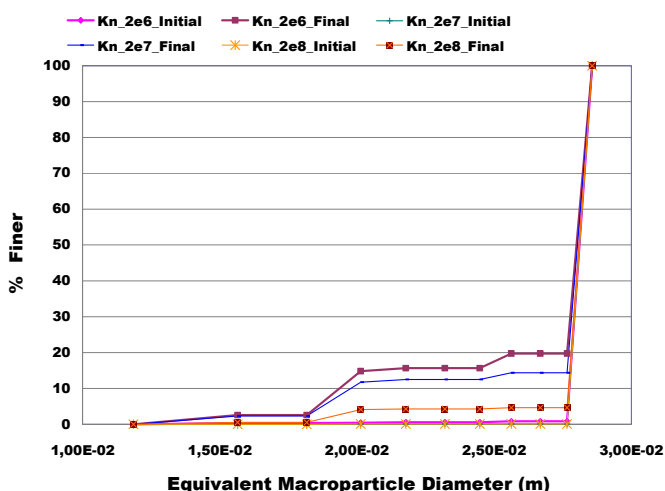


**Fig. 10.** Effect of contact stiffness on the evolution of grain size distribution. Comparison among three different normal stiffness (2e6, 2e7, 2e8 N/m). Sample of 1000 macroparticles using clumps of 14 microparticles. Confining stress: 1.0MPa. Initial porosity: 51%.

### 4.3 Toughness

Particle toughness is a key property in the fracture model selected. Four values were compared:  $1e6 \text{ Pa}\sqrt{\text{m}}$ ;  $1e5 \text{ Pa}\sqrt{\text{m}}$ ;  $1e4 \text{ Pa}\sqrt{\text{m}}$  and  $1e2 \text{ Pa}\sqrt{\text{m}}$ . In all cases a triaxial sample having an initial porosity of 0.51 and a confining stress of 1 MPa was tested. Some results are given in Figures 11, 12 and 13.

Toughness controls the peak strength (Fig. 11) although ‘residual’ values seem to be less affected. Samples having a higher  $Kc$  value exhibit also a stronger dilatancy (Fig. 12). The lower the  $Kc$  value the higher the number of particles ruptured during the test. This is reflected on the calculated grain size distribution at the end of the test (Fig. 13). Crushing in

these samples result in an increase in particles having a equivalent diameter close to 2cm. It is clear that much more deformation energy will be required to achieve an stationary grain size distribution.

These are reasonable results which help to increase the confidence on the model.

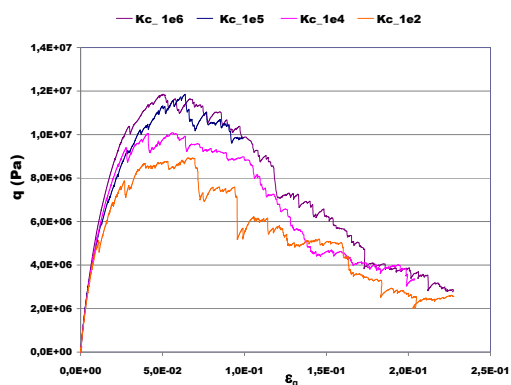


**Fig. 11.** Effect of macroparticle toughness on deviatoric behaviour. Comparison among four different macro-toughness (1e6, 1e5, 1e4, 1e2 Pa√m). Sample of 1000 macroparticles using clumps of 14 microparticles . Confining stress: 1.0MPa. Initial porosity: 51%.

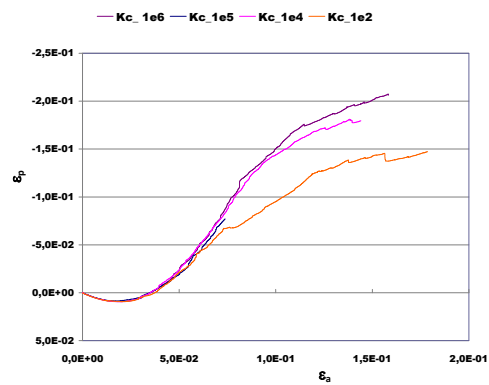


**Fig. 12.** Effect of macroparticle toughness on volumetric behaviour. Comparison among four different macro-toughness (1e6, 1e5, 1e4, 1e2 Pa√m). Sample of 1000 macroparticles using clumps of 14 microparticles . Confining stress: 1.0MPa. Initial porosity: 51%.

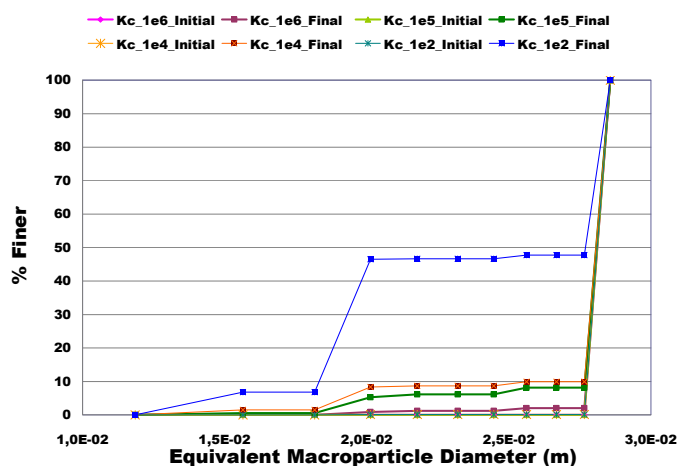


**Fig. 13.** Effect of macroparticle toughness on the evolution of grain size distribution. Comparison among four different macro-toughness (1e6, 1e5, 1e4, 1e2 Pa√m). Sample of 1000 macroparticles using clumps of 14 microparticles . Confining stress: 1.0MPa. Initial porosity: 51%.

#### 4.4 Friction Coefficient

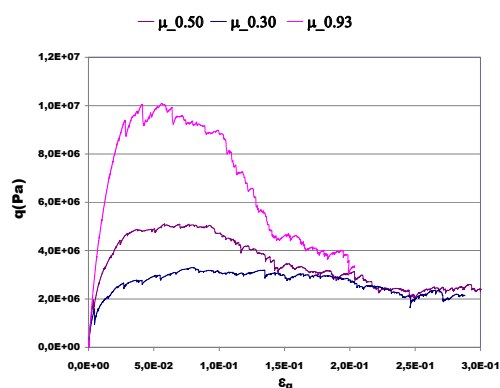
Three samples having particle to particle friction coefficient ( $\mu$ ) equal to 0.93, 0.50 and 0.30 ( $\varphi = 43^\circ; 27^\circ; 17^\circ$ ) were tested in a triaxial experiment. Initial porosity was 51%, the



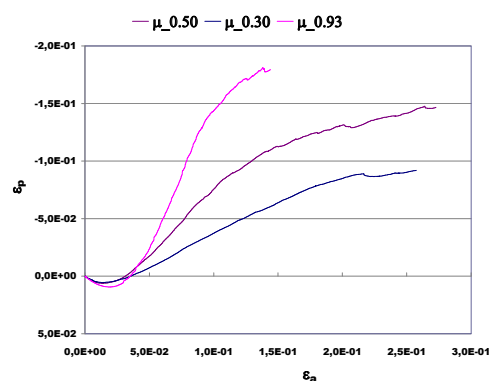
initial confining stress 1 MPa and the toughness of macroparticles was  $1e4 \text{ Pa}\sqrt{\text{m}}$ . The specimen was defined by 970 macroparticles and the initial equivalent diameter was 2.8cm.

Figure 14 shows the deviatoric stress-strain relationship. A similar residual strength for strains in excess of 20% was found. Dilatancy is shown in Figure 15. As expected, dilatancy increases with interparticle friction. In this test most of the particles broken resulted in equivalent particle diameters in the vicinity of 2cm. The sample having the smallest interparticle friction angle exhibited a higher number of failed clumps.

Only a small percentage of particles broke in these tests. More will be said on this aspect in the next section.



**Fig. 14.** Friction coefficient effect on deviatoric behaviour. Comparison among three friction coefficients (0.93, 0.50, 0.30). Sample of 1000 macroparticles using clumps of 14 microparticles. Confining stress: 1.0MPa. Initial porosity: 51%.



**Fig. 15.** Friction coefficient effect on volumetric behaviour. Comparison among three friction coefficients (0.93, 0.50, 0.30). Sample of 1000 macroparticles using clumps of 14 microparticles. Confining stress: 1.0MPa. Initial porosity: 51%.

## 5 RELATIVE HUMIDITY EFFECTS

Investigating the effect of Relative Humidity on rockfill behaviour is one of the main objectives of the work developed. In the cases discussed below the effect of RH is imposed by reducing (suddenly) the  $Kc$  value of macroparticles. This technique simulates the type of triaxial tests reported by Ortega (2010). In some of his strain controlled triaxial tests (Figure 19) samples initially dry were flooded when they reached some given strain level. The vertical strain rate was maintained and the change in vertical stress was recorded. The same technique was repeated in the numerical tests performed.

The macroparticle's aggregate had the following properties: initial porosity = 51%;  $Kc = 1e6 \text{ Pa}\sqrt{\text{m}}$  and  $1e5 \text{ Pa}\sqrt{\text{m}}$ ;  $\mu = 0.93$ . Uniform clump size of 14 microparticles. The confining stress was 1 MPa.

Figures 16 and 17 show the sample response for the three cases:  $Kc_1=1e6 \text{ Pa}\sqrt{\text{m}}$ ,  $Kc_2=1e5 \text{ Pa}\sqrt{\text{m}}$ , and a 'wetting' effect when  $Kc_1$  is reduced suddenly to  $Kc_2$  when the vertical strain reached 5%. The sample experiences a collapse which is reflected in a sudden reduction of the deviatoric stress. Further straining, however, results in a recovery of strength. The reduction in porosity associated with this wetting is irreversible. This is shown in Figure 17, which

provides the variation of porosity during the tests simulated.

Porosity increases because of dilatancy in all cases. However, wetting ( $Kc$  is reduced) results in a transient reduction in porosity. The wetted sample falls into the porosity plot for the specimen having initially a reduced  $Kc$  value.

Figure 18 provides additional information on the evolution of broken macroparticles. A value of  $Kc_1=1e6 \text{ Pa}\sqrt{\text{m}}$  results in a limited breakage of particles. When  $Kc$  is decreased to  $Kc_2=1e5$  the breakage rate increases. The sudden wetting takes the sample from the  $Kc_1$  to  $Kc_2$  curve.

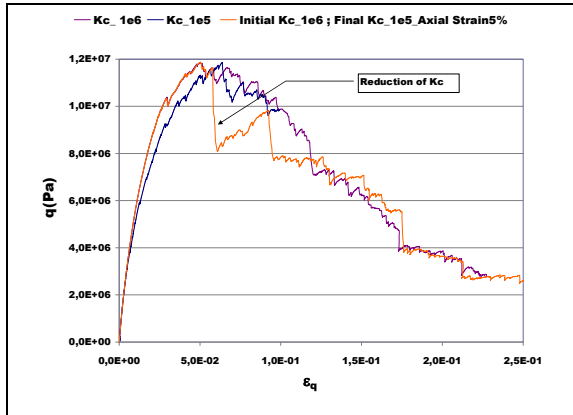


**Fig. 16.** Wetting effect on deviatoric stress behaviour. Sample of 1000 macroparticles using clumps of 14 microparticles. Confining stress: 1.0MPa. Initial porosity: 51%.

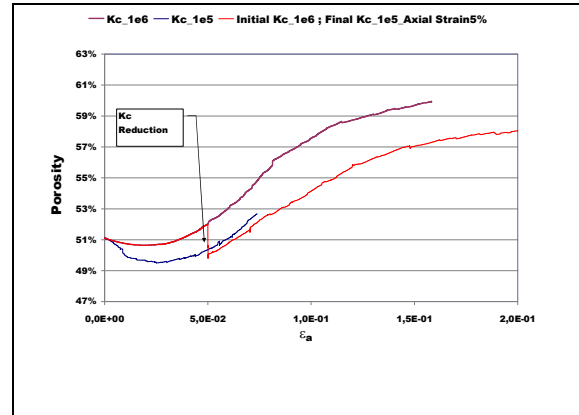


**Fig. 17.** Wetting effect on porosity. Sample of 1000 macroparticles using clumps of 14 microparticles. Confining stress: 1.0MPa. Initial porosity: 51%.

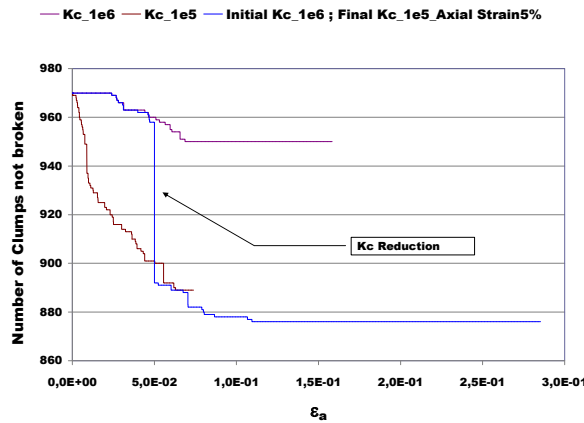


**Fig. 18.** Wetting effect on number of clumps not broken vs axial strain. Sample of 1000 macroparticles using clumps of 14 microparticles. Confining stress: 1.0MPa. Initial porosity: 51%.

Figure 19 shows the results of triaxial tests performed by Ortega (2010) on samples of limestone fragments ranging in size from 1 to 4 cm. The plot shows stress-strain curves for samples maintained at relative humidities of  $RH=10\%$ ;  $50\%$  and  $100\%$ . The driest sample ( $RH=10\%$ ) was fully wetted, once it reached a certain deformation, by means of two processes:

- Specimen flooding by liquid water. The test was then resumed (sample HR10%-Sat-Cut)
- Deviatoric stress was reduced to zero, the sample was flooded and the test was resumed again (sample HR10%-Sat-Desc)

Samples having a smaller RH are stiffer and reach higher strength. The RH=10% sample loaded and then flooded once it was at limiting conditions experienced a sudden reduction in strength which recovered in part as deformation increased. The stress-strain curve approaches now the curve for the RH=100% case.

The discrete model results in Figure 16 and the actual experiments are qualitatively similar. Matching model and experiments require an improved geometrical definition of particles, pore geometry and particle properties.

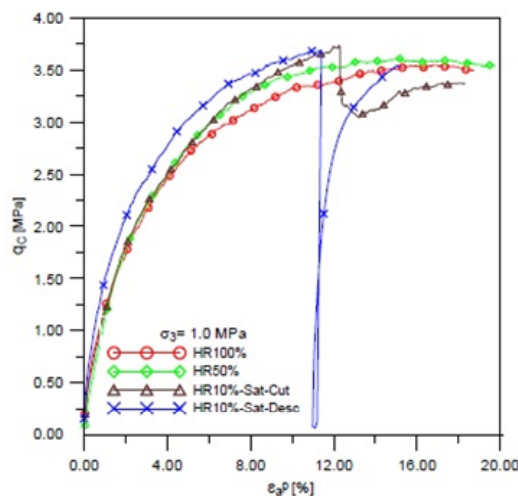


Fig. 19. Triaxial test on limestone rockfill. Stress-strain curve. Confining stress: 1.0MPa. (Ortega, 2010)

## 6 CONCLUDING REMARKS

A key aspect of rockfill behaviour is the particle breakage during the process of deformation under stress levels of common engineering interest. This paper presents some results of an on going research aimed at developing a suitable 'particle' method to analyze rockfill behaviour.

The computer program PFC3D (Itasca, 2008) offers the possibility of grouping individual spherical particles into bigger units (macroparticles) which may simulate the actual shape of rockfill fragments. The possibility of programming internally some relevant phenomena determining the failure (breakage) of individual macroparticles was used to build a dedicated particle-based model which attempts to reproduce real behaviour as revealed by large scale triaxial tests on gravels.

A 'pyramidal' macroparticle shape, made of 14 micro-spheres, was used in the results presented. Other geometries will be explored in future analyses.

The calculated effect of particle shape (to a limited extent), porosity and angle of internal friction follows a consistent pattern.

Particle breakage was related to fracture mechanics concepts. Rock toughness enters as a

natural property. Crack propagation is also controlled by the initial distribution (in the entire sample) of defects and its initial length as well as on stress intensity, current suction (or relative humidity) and time. The effect of some of these variables has been explored. It seems that the model developed has the capability of reproducing the main features of reference real triaxial tests on coarse gravels.

## REFERENCES

- [1] Alonso-Marroquín, F. & Herrmann, H.J. “The incremental response of soils. An investigation using a discrete-element model”. *Journal of Engineering Mathematics*, Vol. 52, 11–34. (2005)
- [2] Atkinson, B.K. “Subcritical crack growth in geological materials”. *J. Geophysical Research*, Vol. 89(B6), 4077-4114. (1984)
- [3] Bagi, K. “Stress and strain in granular assemblies”. *Mechanics of Materials*, Vol. 22, 165-177. (1996)
- [4] Bagi, K. “Microstructural stress tensor of granular assemblies with volume forces”. *J. of Applied Mechanics*, Vol. 66(4), 934-936. (1999)
- [5] Broek, D. *Elementary Engineering Fracture Mechanics*, Martinus Nijhoff Publishers, Dordrecht. (1986)
- [6] Chávez, C. *Estudio del comportamiento triaxial de materiales granulares de tamaño medio con énfasis en la influencia de la succión*, Phd Thesis, Department of Geotechnical Engineering and Geosciences, Technical University of Catalonia. UPC, Barcelona, Spain. (2003)
- [7] Chávez, C. & Alonso, E. “A constitutive model for crushed granular aggregates which includes suction effects”. *Soils and Foundations*, Vol. 43(4), 215-227. (2003)
- [8] Itasca, *Manuals of PFC3D v.4.0: Theory and Background*, Fourth Edition, Itasca Consulting Group Inc, US. (2008)
- [9] Oldecop, L. *Compresibilidad de escolleras. Influencia de la humedad*, Phd Thesis, Department of Geotechnical Engineering and Geosciences, Technical University of Catalonia. UPC, Barcelona, Spain. (2000)
- [10] Oldecop, L. & Alonso, E. “A model for rockfill compressibility”. *Géotechnique*, Vol.51(2), 127-139. (2001)
- [11] Oldecop, L. & Alonso, E. “Testing Rockfill Under Relative Humidity Control”. *Geotechnical Testing Journal*, Vol. 27(3), 269-278. (2004)
- [12] Oldecop, L. & Alonso, E. “Suction effects on rockfill compressibility”. *Géotechnique* Vol. 53, 289–292. (2003)
- [13] Oldecop, L. & Alonso, E. “Theoretical investigation of the time-dependent behaviour of rockfill”. *Géotechnique*, Vol. 57(3), 289–301. (2007)
- [14] Ortega, E. *Comportamiento de materiales granulares gruesos - Efecto de la succión*, Phd Thesis, Department of Geotechnical Engineering and Geosciences, Technical University of Catalonia. UPC, Barcelona, Spain. (2010)
- [15] Saouma, V.E. *Lecture Notes in Fracture Mechanics*, Department of Geotechnical Engineering and Geosciences, Technical University of Catalonia. UPC, Barcelona, Spain. (2007)